Published in final edited form as:

Structure. 2021 March 04; 29(3): 284–291.e3. doi:10.1016/j.str.2020.11.006.

Assessing the Structures and Interactions of γD-Crystallin Deamidation Variants

Alex J. Guseman[1], **Matthew J. Whitley**[1,2], **Jeremy J. González**[1], **Nityam Rathi**[1], **Mikayla Ambarian**[1], **Angela M. Gronenborn**[1,3]

[1]Department of Structural Biology, University of Pittsburgh School of Medicine, Pittsburgh, PA, 15261, USA

[2]current address: Department of Pharmacology and Chemical Biology, University of Pittsburgh School of Medicine, Pittsburgh, PA, 15261, USA

[3]Lead Contact

SUMMARY:

Cataracts involve the deposition of the crystallin proteins in the vertebrate eye lens, causing opacification and blindness. They are associated with either genetic mutation or protein damage that accumulates over the lifetime of the organism. Deamidation of Asn residues in several different crystallins has been observed and is frequently invoked as a cause of cataract. Here, we investigated the properties of Asp variants, deamidation products of γD-crystallin, by solution NMR, X-ray crystallography and other biophysical techniques. No substantive structural or stability changes were noted for all seven Asn to Asp γD-crystallins. Importantly, no changes in diffusion interaction behavior could be detected. Our combined experimental results demonstrate that introduction of single Asp residues on the surface of γD-crystallin by deamidation is unlikely to be the driver of cataract formation in the eye lens.

Graphical Abstract

*Correspondence should be addressed to Angela M. Gronenborn, Department of Structural Biology, University of Pittsburgh School of Medicine, 3501 Fifth Ave., Pittsburgh, PA, 15261, USA. Tel.: (412) 648-9959; Fax: (412) 648-9008; amg100@pitt.edu.

AUTHOR CONTRIBUTIONS

A.J.G., M.J.W. and A.M.G. designed the experiments. A.J.G., M.J.W., J.J.G., N.R. and M.A. prepared samples. M.J.W., N.R. and M.A. conducted crystallographic studies, A.J.G. and J.J.G. performed NMR and light scattering, and A.J.G. DSC experiments. A.J.G., M.J.W., and A.M.G. wrote the manuscript and all authors reviewed and approved the manuscript.

DECLARATION OF INTERESTS

The authors declare no conflict of interest.

Guseman *et al* combined NMR, X-ray crystallography, dynamic light scattering and DSC to demonstrate that single Asn to Asp deamidation has minimal influence on the properties and structure of γD-crystallin.

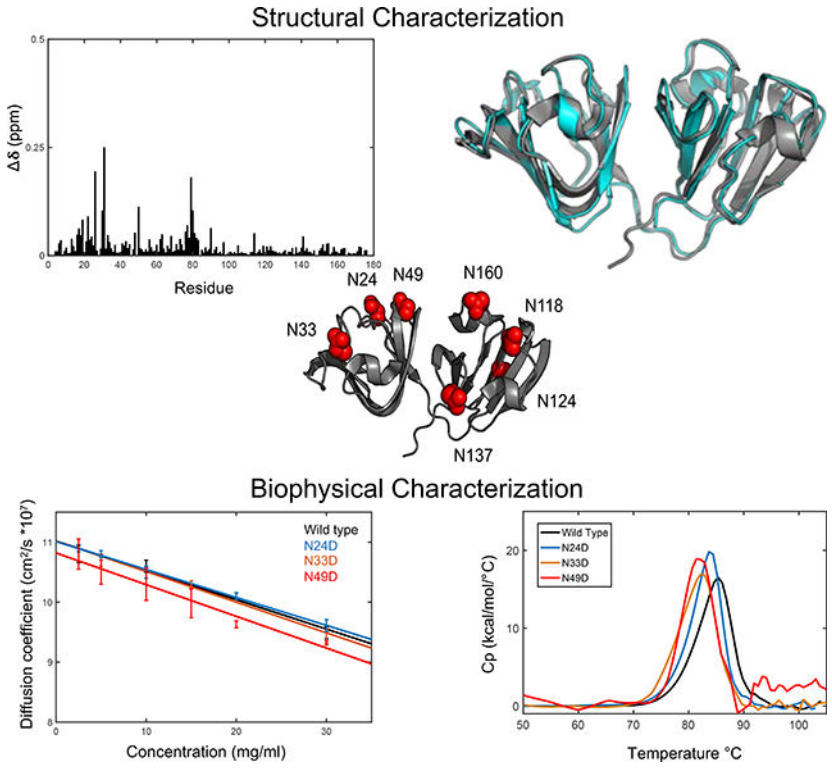

Keywords

γD-crystallin; NMR; X-ray crystallography; deamidation; dynamic light scattering

INTRODUCTION

Over 20 million people are affected by cataracts, the leading cause of blindness world-wide (Lam et al., 2015). Cataract denotes an opacification of the eye lens, brought about by insoluble aggregates of crystallin proteins. The eye lens is a highly unique and specialized organ in the human body, evolved to focus light onto the retina, and at the same time, minimize any scattering of the incoming light (Bloemendal et al., 2004, Zhao et al., 2011a, Zhao et al., 2011b). This is achieved by a uniform distribution of the crystallin proteins at concentrations exceeding 400 g/L, as well as an absence of organelles and large protein machineries in mature lens cells. In essence, a developed lens cell can be viewed as a transparent, densely packed sack of crystallin proteins (Bloemendal et al., 2004, Lam et al., 2015, Sharma and Santhoshkumar, 2009). Since mature lens cells are devoid of protein machines and processes that are necessary for protein synthesis and degradation, essentially no protein turnover takes place. As a result, crystallins are required to be stable and functional over an organism's entire lifespan. They are prototypical members of so-called long-lived proteins (Toyama and Hetzer, 2012, Lynnerup et al., 2008). If damage or other insults compromise their integrity and solubility, aggregation and cataract formation may ensue.

Crystallins are divided into three subfamilies: α, β, and γ crystallins. α-crystallins are large, polydisperse oligomers that resemble heat shock proteins (Jehle et al., 2010) and are thought to serve as chaperones that help to keep β/γ crystallins functional (Ghosh and Chauhan, 2019, Haslbeck et al., 2016). β/γ crystallins are small, extremely stable and soluble proteins, functioning predominantly to safeguard the optical properties of the eye lens. All β/γ crystallins have evolved from a common ancestor, exhibiting homologous amino acid sequences that adopt similar secondary and tertiary structures (Bloemendal et al., 2004, Jaenicke and Slingsby, 2001). They are made up of two domains, each containing two unique antiparallel β-sheet arrangements, known as Greek keys (Basak et al., 2003, Bloemendal et al., 2004). While γ-crystallins are monomeric, β-crystallins can be dimeric or oligomeric (Jaenicke and Slingsby, 2001).

Despite their high stability and the presence of α-crystallin chaperones, the integrity of the crystallins in the eye lens can become compromised with age. In fact, different types of stress such as exposure to ultraviolet radiation, oxidative stress and other insults can result in chemical modifications of the lens proteins, including deamidation, glycation, altered disulfide bond formation and peptide bond cleavage (Sharma and Santhoshkumar, 2009, Hanson et al., 2000, Wilmarth et al., 2006, Serebryany et al., 2018). A leading hypothesis for age-related cataract invokes the accumulation of damaged crystallin proteins, which, in turn, irreversibly aggregate to form insoluble precipitates (Warmack et al., 2019). Proteomic analysis has shown the presence of modified crystallins in aged lenses, and γ-crystallin deamidation has been implicated as a potential driver of cataract formation (Sharma and Santhoshkumar, 2009, Hains and Truscott, 2010, Lampi et al., 2014).

Deamidation is a stochastic chemical process that converts glutamine (Gln) and asparagine (Asn) residues to glutamate or iso-glutamate and aspartate (Asp) or iso-Asp, respectively (Clarke, 1987, Geiger and Clarke, 1987). At neutral pH, Asn deamidation is more common than Gln deamidation and proceeds primarily via a succinimide intermediate, a short-lived ring structure that is formed between the carboxyl side chain and the amide group of the following amino acid in the sequence (Figure 1a). The succinimide ring undergoes hydrolysis, resolving into either aspartate or iso-aspartate. Rates of deamidation of individual amide residues depend upon primary sequence, three-dimensional structure, and solution properties such as pH, temperature, ionic strength, and buffer ions (Robinson, 2002, Warmack et al., 2019). Both deamidation products of Asn reduce the protein's net charge by 1 unit, and, in the case of iso-aspartate, an additional methylene group becomes inserted into the protein backbone following the Cα, thereby causing a distortion in the native connection between peptide planes. In the majority of somatic cells, deamidation is of minimal overall significance since it is a relatively slow kinetic process and normal protein turnover ensures that deamidated proteins are removed and replaced by newly synthesized ones. However, because there is no protein turnover in differentiated lens cells, even a stochastic and kinetically slow process like deamidation can, over time, result in the accumulation of modified crystallins with potentially grave consequences. (Toyama and Hetzer, 2012).

Here, we report an investigation of whether and how the deamidation of Asn to Asp influences crystallin behavior and structure. We chose to evaluate human γD-crystallin since it is the third most abundant γ-crystallin in the lens. Specifically, γD-crystallin represents

~7% of the crystallin protein mass (Lampi et al., 1998, Robinson et al., 2006) and is a major component of the lens nucleus, the oldest part of the lens (Ji et al., 2013a, Bloemendal et al., 2004). Our group has studied human, γD-crystallin extensively (Boatz et al., 2017, Ji et al., 2012, Ji et al., 2013a, Ji et al., 2013b, Whitley et al., 2017), and, in the present study, we changed each of its seven Asn residues to Asp and characterized these deamidation variants by nuclear magnetic resonance (NMR), differential scanning calorimetry (DSC), dynamic light scattering (DLS), and X-ray crystallography. Surprisingly, no substantive stability or structural changes were noted in any of the variants, and no changes in diffusion interaction behavior could be detected.

RESULTS:

Each of the seven Asn residues in human γD-crystallin (Figure 1b) were mutated to Asp and the proteins were structurally characterized. To this end, ^{1}H-^{15}N HSQC spectra were recorded and used as a “fingerprint” of the proteins’ three-dimensional structures (Forman-Kay et al., 1992). As evidenced from the differences in amide chemical shifts for all the mutants, compared to wild-type γD-crystallin (Figure 2), no large differences (>0.5 ppm) are noted for any variant, apart from N33D. Small deviations from the wild-type resonance frequencies are noted for amino acids close to the mutation site, and, in general, these changes are restricted to the domains that harbor the mutation site. Thus, for N24D, N33D and N49D, essentially no chemical shift changes are observed for any residues in the C-terminal domain (CTD). Likewise, for the N118D, N124D, N137D and N160D variants that possess mutations in the CTD, no substantive chemical shift changes are seen for amide resonances of amino acids in the N-terminal domain (NTD). Interestingly, for N33D, we observed non-negligible chemical shift changes throughout the NTD, with 11 amide resonances exhibiting differences of 0.2 ppm to 1.15 ppm, compared to their wild-type counterparts. The largest shift differences are associated with residues R32 and S34, which experience amide proton shift differences of −0.022 and 0.23 ppm, respectively, and ^{15}N shift differences of −1.30 and 2.78 ppm, respectively (Figure S1). N33 is the first amino acid in β-strand 3 of the N-terminal domain and participates in a hydrogen bonding network involving Y6 in β-strand 1 across the β-sheet structure of the Greek key motif. Two further H-bonds are present between the side chain amino group of N33 and the backbone carboxyl of E7 and the D73 side chain in the loop following the short α-helix. Therefore, the effect of the N33D mutation could easily propagate to the neighboring structural elements via this hydrogen bonding network. Indeed, the importance of the conserved sequence signature of Y6, E7, F11, G13, and S34 of motif 1 in the arrangement of the first Greek key in the crystallin domain fold has been emphasized previously (Jaenicke and Slingsby, 2001).

In addition to using NMR for characterizing the structural changes induced by the Asn to Asp mutation, we also employed crystallography. Although crystallization trials were carried out for all the deamidation variants, diffraction quality crystals were obtained for only two, N124D and N160D, up to now. Their crystal structures were solved to 1.15 Å and 1.2 Å, respectively (Table 1). The crystal structures confirmed the NMR findings that only very small conformational changes are present in these two variants: Superposition of the NTD (residues 1–81) and CTD (residues 89–17) of the N124D mutant (cyan, Figure 3 left) onto those of wild-type γD-crystallin (grey, Fig. 4 left) yielded average pairwise backbone

r.m.s.d. values of 0.279 Å and 0.182 Å, respectively. For the N160D mutant (green, Figure 3 right), average pairwise backbone r.m.s.d. values of 0.300 Å and 0.219 Å, are seen for the NTD and CTD coordinates, respectively. As an aside, the two molecules of N160D in the asymmetric unit exhibit an average pairwise backbone r.m.s.d. value of 0.269 Å, validating that the structures are essentially identical.

We further investigated whether any of the Asn to Asp mutants exhibited significantly reduced thermodynamic stability compared to wild-type γD-crystallin. To this end, DSC was used. Unfortunately, all the mutant crystallins, as well as the wild-type protein, displayed visible precipitation upon thermal unfolding, which precluded the extraction of accurate thermodynamic parameters. However, the thermograms (Figure S2) still yielded reliable values for the melting temperature. For all the investigated crystallins, the apparent T_m values range from 80 to 85 °C, with a T_m of 81.2 °C for wild-type (Table 2). Only one mutant, N137D, exhibited a lower melting temperature than wild-type γD-crystallin; all others were higher, with N160D the highest. All T_m values are within 3.1 °C of the average value of 82.4 °C, just twice the standard deviation (±1.61 °C).

In addition to thermal stability, reversible association in solution, also called colloidal stability, was evaluated by measuring the diffusivity, or diffusion interaction parameter (DIP) of the different Asn to Asp mutants by DLS. This parameter is dominated by weak, attractive forces related to surface charges. Since each individual Asn to Asp change alters the charge in seven different locations on the γD-crystallin surface, the DIP represents an ideal measure for effects imparted by charge-mediated association. Wild-type γD-crystallin and all Asn to Asp mutants yielded DIP values of similar magnitude, between −3 mL/g and −6 mL/g (Figure 4, Table 3). All values lie within the error range of the value for wild-type γD-crystallin, namely −4 ± 1 mL/g. Thus, no significant changes in weak associative interactions for the different variants in solution were detected over a ten-fold change in protein concentration, ranging from 2.5–30 mg/ml.

Since the interaction between proteins is governed by the respective protein surfaces, we calculated the solvent accessible surface area (SASA) for all heavy atoms of the seven Asn residues in the solution NMR structure PDB ID 2KLJ (Wang et al., 2009) using the protSA server (Estrada et al., 2009) for assessing the potential impact of Asp mutations. All Asn residues are located on the surface of the protein (Figure 2 top left) and are largely solvent exposed, with the exceptions of N33 and N124 where only the amino or carbonyl side chain groups are accessible to solvent (Figure S3). Uniquely, N33 was the least solvent exposed with just the side chain carboxyl oxygen (OD1) of N33 possessing 5 $Å^2$ of SASA.

DISCUSSION:

Deamidation of Asn residues is a common modification found in long-lived proteins and is often invoked as a cause for age-related cataracts (Hains and Truscott, 2010, Hanson et al., 2000, Lampi et al., 2012, Lampi et al., 2016, Lampi et al., 2001, Lampi et al., 2014, Michiel et al., 2010, Srivastava and Srivastava, 2003, Warmack et al., 2019). Since structure and stability are key attributes for safeguarding function, we performed a comprehensive study of the seven possible end products of γD-crystallin deamidation. Both NMR and

crystallographic characterizations of the seven Asn to Asp mutants revealed minimal structural perturbations. Only N33D exhibited local chemical shift changes (Figure S4). Although initially surprising, our findings may be explained by an analysis of the γ-crystallin protein family sequences and the specific locations of the implicated residues in the protein structure. Alignment of the protein sequences of the five γ-crystallin paralogs shows that only three of the seven Asn residues (N33, N49, and N137) are strictly conserved (Figure 1b). N24 and N160 of γD-crystallin are D24 (in γS-crystallin) and D160 (in γA-crystallin and γC-crystallin). This suggests that at positions 24 and 160, Asp residues are tolerable, even if the neighboring amino acids are not completely identical to those in γD-crystallin. As a consequence, no gross structural changes would be expected. This notion is consistent with our finding that only N33D, one of the conserved Asn residues, exhibited significant chemical shift changes in the ^{1}H-^{15}N HSQC spectrum.

Why only the N33D mutant exhibited notable ^{1}H,^{15}N amide chemical shift changes can be explained by our SASA data and the H-bond networks inferred from the X-ray structures. Our SASA analysis revealed that N33 is buried (Figure S3). Therefore, for this particular amino acid, a change from Asn to Asp could cause a local conformational pertubation, which may manifest itself in chemical shift differences, especially if the side chain amino group was involved in structurally relevant interactions. We also inspected the seven Asn residues and their local environments in the X-ray structure of wild-type γD-crystallin (PDB 1HK0 (Basak et al., 2003)). N33 is unique because it is involved in a H-bonding network across the first Greek key in the N-terminal domain (Figure S5). The NH_2 group of the N33 side chain donates a H-bond to the backbone carbonyl of E7, as well as to the side chain carboxyl of D73. These interactions will no longer be possible in the Asn to Asp mutant and, as a result, chemical shift changes for E7 and D73 would be expected in the mutant spectrum. This is indeed the case. Further contacts are present between the backbone amide of N33 and the Y6 backbone carbonyl, H-bonding across a β-sheet, as well as the N33 backbone carbonyl and the adjacent S34 side chain. It appears that without the amino group, which links two structural elements on either side, the backbone conformation of the N33-S34 unit is affected. This is consistent with the S34 amide group exhibiting the largest chemical shift difference upon Asn to Asp mutation.

For the N124D mutant, we inspected the conformational details in our current X-ray structure of this variant and compared them to those in the X-ray structure of wild-type γD-crystallin (PDB ID 1HK0, (Basak et al., 2003)). The two β-sheet backbone H-bonds between N/D124 and R90 are preserved in both structures (Figure S6), suggesting that no significant chemical shift changes of amide resonances will be caused. In contrast, in the D124 mutant structure, the H-bond between the amino group of the N124 side chain and the backbone carbonyl of G148 that is seen in wild-type γD-crystallin (Figure S6) is no longer present.

We also compared the X-ray structures of the N160D variant and the wild-type γD-crystallin (PDBID 1HK0) in relation to the NMR results. The N160D mutant exhibited minimal amide chemical shift changes in the ^{1}H,^{15}N HSQC spectrum (Figure 2), with the exceptions of V163 and G164, whose amide resonances displayed composite chemical shift differences of 0.522 and 0.23 ppm, respectively. These residues are located in a loop close to

the mutation site and adjacent to R162 in the X-ray structure, which can form a salt bridge with E134 in the N160D mutant (Figure S7). Again, the crystallographic details match the NMR data (Figure 3). The potential additional interaction seen in one of the two molecules in the N160D crystal structure may explain the 4.3°C increase in apparent T_m.

Interestingly, our results with respect to structure are similar to observations on congenital cataract variants of γD-crystallin, including three P23 variants, R76S, V75D, W42R as well as other mutants (McManus et al., 2007, Whitley et al., 2017, Ji et al., 2012, Ji et al., 2013a, Ji et al., 2013b). At position 23, P23S and P23V exhibit minimal structural changes (McManus et al., 2007) as does P23T variant (Ji et al., 2013b). Finally, R76S, W42R, and V75D were also characterized by our group and none exhibited gross structural changes (Ji et al., 2012, Ji et al., 2013a, Whitley et al., 2017). Combining all these findings on the atomic structures of these variants and the current deamidated γD-crystallin variants, reinforces the notion that γD-crystallin is robust in its ability to maintain its overall structure.

Given that only minimal structural differences were noted for the Asn to Asp mutants of γD-crystallin, the thermodynamic stability or reversible aggregation properties could have been significantly affected in the mutants. Such changes, however, were not observed, and only small thermal stability differences, all within ±5 °C, were noted. These differences in an otherwise exceedingly stable protein are too small to be considered as a rationale for cataractogenesis. Additionally, these results are contrary to data on Gln deamidation at positions 54 or 143, where Gln residues make key interdomain contacts and where the introduction of Glu results in destabilization of the protein (Flaugh et al., 2006). While our observed changes in structure and thermodynamic stability of γD crystallin are minimal, deamidation in other crystallins can influence the protein's aggregation propensity, as shown for γS-crystallin, even if only minimal effects on structure and stability are seen (Brubaker et al., 2011). We, therefore, carefully investigated whether we could observe any such changes by analyzing DIP values that report on colloidal stability (Saluja et al., 2010, Lehermayr et al., 2011). No significant changes in DIP, a proxy for the second virial coefficient, was found. Therefore, the introduction of a negative charge by deamidation of any of the seven Asn residues in γD-crystallin variants does not significantly influence the self-interaction behavior of these molecules in solution.

Intriguingly, our results differ from those observed for γS-crystallin and β-crystallins, suggesting that not all crystallins are equally affected by deamidation. For example, deamidation does not change the structure of γS-crystallin but does alter its stability, aggregation propensity and dynamics (Ray et al., 2016, Pande et al., 2015, Takemoto and Boyle, 2000, Forsythe et al., 2019, Vetter et al., 2020). For β-crystallins, deamidation can cause compaction, disrupt heterodimer formation, and promote formation of higher order oligomers (Takata et al., 2008, Takata et al., 2010, Lampi et al., 2012, Lampi et al., 2016, Lampi et al., 2001, Michiel et al., 2010, Lampi et al., 2002, Lampi et al., 2006). Here, for γD-crystallin, no significant difference in stability or aggregation propensity was observed.

Overall, our data demonstrate that the aspartate product of Asn deamidation has minimal impact on the structure and biophysical properties of γD-crystallin. These results suggest

that γD-crystallin can tolerate a single deamidation while maintaining its structure and function. However, we cannot exclude synergistic effects of additional deamidations or modifications, such as oxidation, on the structural or biophysical properties of the protein. To further elucidate the influences of deamidation or any modification, the lens environment has to be taken into account since the behavior of proteins in a crowded environment can be different from that in dilute solution, especially with respect to folding or protein-protein interactions (Guseman et al., 2018, Monteith et al., 2015).

CONCLUSIONS:

Systematic biophysical analysis of γD-crystallin surface deamidation variants indicates that single Asn to Asp amino acid changes in γD-crystallin are unlikely to drive cataract formation. Both NMR and crystallographic data demonstrate that, at most, very minor conformational changes are induced, but these do not result in decreased protein stability or altered self-association behavior. Even if such changes are frequently observed in proteomic analyses of aged lenses, irrespective of whether they exhibit cataract (Hains and Truscott, 2010), our results serve as a cautionary tale for generally implicating deamidation from Asn to Asp in cataractogenesis. Whether any of the other intermediates or deamidation products in a particular α, β or γ-crystallin contribute to, or cause, cataracts will require further detailed studies.

STAR METHODS

Resource Availability

Lead Contact—Further information and reagent requests should be addressed to lead contact Angela Gronenborn (amg100@pitt.edu).

Material availability: This study did not generate new unique reagents.

Data availability: Atomic coordinates for the N124D and N160D γD-crystallin variants are deposited in the RCSB PDB with accession codes 6W5B and 6WCY, respectively.

Experimental Model and Subject Details

Bacterial Cell Culture—BL21(DE3) cells obtained from New England BioLabs (cat #C2527H) were used for expression of human γD-crystallin and Asp variants. Cells harboring the transformed γD-crystallin plasmid were cultured in LB broth or modified M9 minimal medium with 100 μg/ml of carbenicillin at 37°C.

Method Details—Expression and purification: Human γD-crystallin and the Asp variants were expressed and purified as previously described (Ji et al., 2012). In short, BL21(DE3) *E. coli* cells were transformed with a pET14b vector containing either the WT *CRYGD* gene or a deamidation variant. Cells harboring the transformed γD-crystallin plasmid were cultured in LB broth or modified M9 minimal medium containing 1 g/L $^{15}NH_4Cl$ and grown to an absorbance (A_{600}) between 0.6–0.8, at which time 1 mM IPTG was added, and protein expression was continued for 4 hours. Cells were harvested by centrifugation and resuspended in Q_a buffer (20 mM Tris pH 8.0, 1mM EDTA, 1 mM DTT). Cells were lysed

by microfluidization, lysates were cleared by centrifugation at 39,000*g* for 40 minutes, and the supernatant was collected and filtered through a 0.22 μm filter. The cleared supernatant was passed over a HiTrap Q HP anion exchange column pre-equilibrated at 4°C, and the flow through was collected and dialyzed overnight into 4 L of S_a buffer (20 mM MES pH 6.0, 1mM EDTA, 1 mM DTT). Post dialysis, aggregates were removed by centrifugation at 39,000*g* for 20 minutes, and the supernatant was passed through a 0.22 μm filter and loaded on a HiTrap HP SP cation exchange column in S_a buffer. Protein was eluted using a linear gradient of 0–50% S_b (20 mM MES pH 6.0, 1mM EDTA, 1 mM DTT, 1 M NaCl) over 10 column volumes. 5 mL fractions were collected, and fractions that contained γD-crystallin were pooled and concentrated to <5 mL using an Amicon spin concentrator. The final purification involved gel filtration over an S75 16/600 column in S_a buffer. Fractions were analyzed by SDS PAGE, and those containing pure γD-crystallin were collected, pooled, and concentrated to less than 2 mL total volume. Protein concentration was determined using a Nanodrop ND-1000 and a molar extinction coefficient of 40680 M^{-1} cm^{-1}.

NMR Spectroscopy: All NMR experiments were carried out at 25°C using a Bruker AVANCE 800 MHz spectrometer equipped with a z-axis gradient, triple resonance cryoprobe. 2D ^{1}H-^{15}N HSQC spectra were recorded on samples containing 150 μM protein in 20 mM MES buffer, 1 mM EDTA, 1 mM TCEP, pH 6.0 and 10% D_2O. Resonance assignments were carried out in NMRFAM-SPARKY (Lee et al., 2014) and crosschecked against previously published assignments for the wild-type protein (Ji et al., 2012). Chemical shift differences for the mutant variants were calculated according to

$$\Delta\delta: \sqrt{\left(\delta H_v - \delta H_{wt}\right)^2 + \left(\frac{\delta N_v - \delta N_{wt}}{6}\right)^2}$$

(Williamson, 2013).

Crystallization of γD-Crystallin Asp Variants: The N124D and N160D deamidation mutants were concentrated to 10 mg/mL in size exclusion buffer. Crystallization trials were performed using sitting drop vapor diffusion. An initial crystallization hit with N124D was obtained in 0.2 M magnesium chloride hexahydrate, 0.1 M Tris (pH 7.0), and 10% w/v PEG 8000; these crystals were crushed and diluted in the same solution to serve as a seed stock for random matrix microseeding (rMMS) trials (D'Arcy et al., 2007). Diffraction quality crystals were obtained in a crystallization solution consisting of 0.2 M lithium sulfate, 0.1 M phosphate-citrate (pH 4.2), and 20% w/v PEG 1000. Crystals were harvested, vitrified in liquid nitrogen without additional cryoprotection and used for data collection. For N160D, initial poor-quality plate-type crystals were obtained in 25% w/v PEG 3350, 0.1 M Bis-Tris (pH 5.5), and 0.2 M ammonium sulfate. Crushed crystals were used for rMMS, which yielded numerous crystals of high quality. Final crystals, grown in 0.1 M succinic acid (pH 7.0) and 15% w/v PEG 3350, were harvested, vitrified in liquid nitrogen without additional cryoprotectant, and used for data collection.

X-ray Diffraction and Structure Determination: Diffraction data for N124D were recorded at the GM/CA beamline 23-ID-D of the Advanced Photon Source at Argonne

National Laboratory (Lemont, IL, USA). The X-ray wavelength was 0.8856 Å, and 1800 images were recorded at an oscillation width of 0.2° per image. Diffraction data for N160D were recorded at SER-CAT beamline 22-ID of the Advanced Photon Source at Argonne National Laboratory. Using X-rays of wavelength 1.0 Å, 720 diffraction images were recorded at an oscillation width of 0.5° per image. Data reduction and scaling were performed with XDS (Kabsch, 2010). N124D crystallized in the primitive orthorhombic space group $P2_12_12_1$ with a single molecule in the asymmetric unit. N160D also crystallized in space group $P2_12_12_1$, but with two molecules in the asymmetric unit. For each mutant, phases were determined by molecular replacement in Phaser (McCoy et al., 2007), using the WT structure (PDB 1HK0) as the search model. Before molecular replacement, the four tryptophan side chains in the search model were truncated to alanine, and the presence of side chain density for these tryptophans in the molecular replacement solutions was used to validate their correctness. The molecular replacement solutions were rebuilt using Phenix AutoBuild (Terwilliger et al., 2008) and subjected to multiple iterations of manual model correction in Coot (Emsley and Cowtan, 2004) and automated refinement in Phenix (Liebschner et al., 2019, Adams et al., 2010). Riding hydrogens were added to both mutant models for refinement. Anisotropic atomic displacement parameters (ADP) were refined for N124D. For N160D, refinement of anisotropic ADP led to a large decrease in R_{work} but a much smaller decrease in R_{free}. To avoid overfitting, refinement of anisotropic ADP was abandoned for this mutant in favor of a simpler TLS model, which led to a similar decrease in both R_{work} and R_{free}. Non-crystallographic symmetry restraints were also used during N160D refinement. Final refinement for the N124D and N160D models was to a resolution of 1.15 and 1.20 Å, respectively. Full data collection and refinement statistics are provided in Table 1. The diffraction data and refined models for N124D and N160D γD-crystallin were deposited in the Protein Data Bank under accession codes 6W5B and 6WCY, respectively.

Dynamic Light Scattering: Purified human γD-crystallin was concentrated to >50 mg/mL in 20 mM MES buffer, 1mM EDTA, 1 mM DTT, pH 6.0. Buffer and protein solutions were filtered through a 0.01 μm filter, and concentrations were determined spectroscopically, using an extinction coefficient of 40680 M^{-1} cm^{-1}. DLS was performed using a DynaPro Plate Reader III (Wyatt Technology, Santa Barbara, CA) in a 384 well plate format at 298 K. Samples (60 μL) at protein concentrations between 2.5 and 30 mg/mL were prepared, and triplicates of 20 μL each were measured. Ten acquisitions were collected for each sample, and data for the ten acquisitions were averaged. Data were analyzed in Dynamics 7.1.7, plotted in MatLab and fit to $D = (D_0 + D_0 k_D c)$, with D the diffusion coefficient, D_0 the diffusion coefficient at infinite dilution, k_D the diffusion interaction parameter, and c the protein concentration, uncertainties reflect the 95% confidence interval of the fit and are reported in Table 3.

Differential Scanning Calorimetry: Thermal unfolding was performed on a Microcal VP-DSC microcalorimeter. Crystallin variants were dialyzed twice against five liters of water. The dialysis water was filtered and saved for recording the reference baseline. The temperature was ramped from 25–110°C per scan at 90 °C/hour. The data were analyzed using the Origin DSC software package.

Quantification and statistical analysis

Details of statistical analysis can be found in the methods description for each technique used. In Short, DLS data was analyzed in Dynamics 7.1.7 and plotted in MatLab which was also used to fit the data as described in the methods section, the uncertainties reflect the 95% confidence interval of the fit and is reported in Table 3. DSC thermograms were analyzed in Origin DSC software package to determine T_m and are reported in Table 2. Finally, a detailed description of the statistics for the X-ray structure determination are stated in the methods section and reported in Table 1.

Supplementary Material

Refer to Web version on PubMed Central for supplementary material.

ACKNOWLEDGEMENTS:

Members of the Gronenborn laboratory are gratefully acknowledged for assistance and insightful comments and George Makhatadze for discussions on differential scanning calorimetry. We thank Doug Bevan for computer, Mike Delk for NMR and Doowon Lee for X-ray technical support, and Teresa Brosenitsch for critically reading the manuscript.

FUNDING:

This work was supported by National Institutes of Health grants R01 EY030057. Alex J. Guseman is a Merck fellow of the Life Sciences Research Foundation and holds a Postdoctoral Enrichment Program Award from the Burroughs Wellcome Fund.

REFERENCES

ADAMS PD, AFONINE PV, BUNKOCZI G, CHEN VB, DAVIS IW, ECHOLS N, HEADD JJ, HUNG L-W, KAPRAL GJ, GROSSE-KUNSTLEVE RW, MCCOY AJ, MORIARTY NW, OEFFNER R, READ RJ, RICHARDSON DC, RICHARDSON JS, TERWILLIGER TC & ZWART PH 2010. Phenix: A comprehensive python-based system for macromolecular structure solution. Acta Crystallogr., Sec. D., 66, 213–221.

BASAK A, BATEMAN O, SLINGSBY C, PANDE A, ASHERIE N, OGUN O, BENEDEK GB & PANDE J 2003. High-resolution X-ray crystal structures of human γD crystallin (1.25 Å) and the R58H mutant (1.15 Å) associated with aculeiform cataract. J. Mol. Biol, 328, 1137–1147. [PubMed: 12729747]

BLOEMENDAL H, DE JONG W, JAENICKE R, LUBSEN NH, SLINGSBY C & TARDIEU A 2004. Ageing and vision: Structure, stability and function of lens crystallins. Prog. Biophys. Mol. Biol, 86, 407–485. [PubMed: 15302206]

BOATZ JC, WHITLEY MJ, LI M, GRONENBORN AM & VAN DER WEL PCA 2017. Cataract-associated P23T γD-crystallin retains a native-like fold in amorphous-looking aggregates formed at physiological pH. Nat. Commun, 8, 15137. [PubMed: 28474685]

BRUBAKER WD, FREITES JA, GOLCHERT KJ, SHAPIRO RA, MORIKIS V, TOBIAS, DOUGLAS J. & MARTIN RW 2011. Separating instability from aggregation propensity in γS-crystallin variants. Biophys. J, 100, 498–506. [PubMed: 21244846]

CLARKE S 1987. Propensity for spontaneous succinimide formation from aspartyl and asparaginyl residues in cellular proteins. Int. J. Pept. Protein Res, 30, 808–821. [PubMed: 3440704]

D'ARCY A, VILLARD F & MARSH M 2007. An automated microseed matrix-screening method for protein crystallization. Acta Crystallogr., Sec. D, 63, 550–554.

EMSLEY P & COWTAN K 2004. Coot: Model-building tools for molecular graphics. Acta Crystallogr., Sec. D, 60, 2126–2132.

ESTRADA J, BERNADÓ P, BLACKLEDGE M & SANCHO J 2009. ProtSA: A web application for calculating sequence specific protein solvent accessibilities in the unfolded ensemble. BMC Bioinf, 10, 104.

FLAUGH SL, MILLS IA & KING J 2006. Glutamine deamidation destabilizes human γD-crystallin and lowers the kinetic barrier to unfolding. J. Biol. Chem, 281, 30782–30793. [PubMed: 16891314]

FORMAN-KAY JD, CLORE GM, STAHL SJ & GRONENBORN AM 1992. ^{1}H and ^{15}N resonance assignments and secondary structure of the human thioredoxin C62A, C69A, C73A mutant. J. Biomol. NMR, 2, 431–445. [PubMed: 1422155]

FORSYTHE HM, VETTER CJ, JARA KA, REARDON PN, DAVID LL, BARBAR EJ & LAMPI KJ 2019. Altered protein dynamics and increased aggregation of human γS-crystallin due to cataract-associated deamidations. Biochemistry, 58, 4112–4124. [PubMed: 31490062]

GEIGER T & CLARKE S 1987. Deamidation, isomerization, and racemization at asparaginyl and aspartyl residues in peptides. Succinimide-linked reactions that contribute to protein degradation. J. Biol. Chem, 262, 785–794. [PubMed: 3805008]

GHOSH KS & CHAUHAN P 2019. Crystallins and their complexes. In: HARRIS JR & MARLES-WRIGHT J (eds.) Macromolecular protein complexes ii: Structure and function. Cham: Springer International Publishing.

GUSEMAN AJ, SPEER SL, PEREZ GONCALVES GM & PIELAK GJ 2018. Surface charge modulates protein–protein interactions in physiologically relevant environments. Biochemistry, 57, 1681–1684. [PubMed: 29473738]

HAINS PG & TRUSCOTT RJW 2010. Age-dependent deamidation of lifelong proteins in the human lens. Invest. Ophthalmol. Visual Sci, 51, 3107–3114. [PubMed: 20053973]

HANSON SRA, HASAN A, SMITH DL & SMITH JB 2000. The major in vivo modifications of the human water-insoluble lens crystallins are disulfide bonds, deamidation, methionine oxidation and backbone cleavage. Exp. Eye Res, 71, 195–207. [PubMed: 10930324]

HASLBECK M, PESCHEK J, BUCHNER J & WEINKAUF S 2016. Structure and function of α-crystallins: Traversing from in vitro to in vivo. Biochim. Biophys. Acta, 1860, 149–166. [PubMed: 26116912]

JAENICKE R & SLINGSBY C 2001. Lens crystallins and their microbial homologs: Structure, stability, and function. Crit. Rev. Biochem. Mol. Biol, 36, 435–499. [PubMed: 11724156]

JEHLE S, RAJAGOPAL P, BARDIAUX B, MARKOVIC S, KÜHNE R, STOUT JR, HIGMAN VA, KLEVIT RE, VAN ROSSUM B-J & OSCHKINAT H 2010. Solid-state NMR and SAXS studies provide a structural basis for the activation of αB-crystallin oligomers. Nat. Struct. Mol. Biol, 17, 1037–1042. [PubMed: 20802487]

JI F, JUNG J & GRONENBORN AM 2012. Structural and biochemical characterization of the childhood cataract-associated R76S mutant of human γD-crystallin. Biochemistry, 51, 2588–2596. [PubMed: 22394327]

JI F., JUNG J., KOHARUDIN LMI. & GRONENBORN AM. 2013a. The human W42R γD-crystallin mutant structure provides a link between congenital and age-related cataracts. J. Biol. Chem., 288, 99–109. [PubMed: 23124202]

JI F, KOHARUDIN LMI, JUNG J & GRONENBORN AM 2013b. Crystal structure of the cataract-causing P23T γD-crystallin mutant. Proteins: Struct., Funct., Bioinf, 81, 1493–1498.

KABSCH W 2010. Xds. Acta Crystallogr., Sec. D, 66, 125–132.

LAM D, RAO SK, RATRA V, LIU Y, MITCHELL P, KING J, TASSIGNON M-J, JONAS J, PANG CP & CHANG DF 2015. Cataract. Nat. Rev. Disease, 1, 15014.

LAMPI KJ, AMYX KK, AHMANN P & STEEL EA 2006. Deamidation in human lens βB2-crystallin destabilizes the dimer. Biochemistry, 45, 3146–3153. [PubMed: 16519509]

LAMPI KJ, FOX CB & DAVID LL 2012. Changes in solvent accessibility of wild-type and deamidated βB2-crystallin following complex formation with αA-crystallin. Exp. Eye Res, 104, 48–58. [PubMed: 22982024]

LAMPI KJ, KIM YH, BÄCHINGER HP, BOSWELL BA, LINDNER RA, CARVER JA, SHEARER TR, DAVID LL & KAPFER DM 2002. Decreased heat stability and increased chaperone requirement of modified human betab1-crystallins. Mol Vis, 8, 359–66. [PubMed: 12355063]

LAMPI KJ, MA Z, HANSON SRA, AZUMA M, SHIH M, SHEARER TR, SMITH DL, SMITH JB & DAVID LL 1998. Age-related changes in human lens crystallins identified by two-dimensional electrophoresis and mass spectrometry. Exp. Eye Res, 67, 31–43. [PubMed: 9702176]

LAMPI KJ, MURRAY MR, PETERSON MP, ENG BS, YUE E, CLARK AR, BARBAR E & DAVID LL 2016. Differences in solution dynamics between lens β-crystallin homodimers and heterodimers probed by hydrogen–deuterium exchange and deamidation. Biochim. Biophys. Acta, 1860, 304–314. [PubMed: 26145577]

LAMPI KJ, OXFORD JT, BACHINGER HP, SHEARER TR, DAVID LL & KAPFER DM 2001. Deamidation of human βB1 alters the elongated structure of the dimer. Exp. Eye Res, 72, 279–288. [PubMed: 11180977]

LAMPI KJ, WILMARTH PA, MURRAY MR & DAVID LL 2014. Lens β-crystallins: The role of deamidation and related modifications in aging and cataract. Prog. Biophys. Mol. Biol, 115, 21–31. [PubMed: 24613629]

LEE W, TONELLI M & MARKLEY JL 2014. NMRFAM-SPARKY: Enhanced software for biomolecular NMR spectroscopy. Bioinformatics, 31, 1325–1327. [PubMed: 25505092]

LEHERMAYR C, MAHLER H-C, MÄDER K & FISCHER S 2011. Assessment of net charge and protein-protein interactions of different monoclonal antibodies. J. Pharm. Sci, 100, 2551–2562. [PubMed: 21294130]

LIEBSCHNER D, AFONINE PV, BAKER ML, BUNKOCZI G, CHEN VB, CROLL TI, HINTZE B, HUNG L-W, JAIN S, MCCOY AJ, MORIARTY NW, OEFFNER RD, POON BK, PRISANT MG, READ RJ, RICHARDSON JS, RICHARDSON DC, SAMMITO MD, SOBOLEV OV, STOCKWELL DH, TERWILLIGER TC, URZHUMTSEV AG, VIDEAU LL, WILLIAMS CJ & ADAMS PD 2019. Macromolecular structure determination using X-rays, neutrons and electrons: Recent developments in phenix. Acta Crystallogr., Sec. D, 75, 861–877.

LYNNERUP N, KJELDSEN H, HEEGAARD S, JACOBSEN C & HEINEMEIER J 2008. Radiocarbon dating of the human eye lens crystallines reveal proteins without carbon turnover throughout life. PLoS One, 3, e1529. [PubMed: 18231610]

MCCOY AJ, GROSSE-KUNSTLEVE RW, ADAMS PD, WINN MD, STORONI LC & READ RJ 2007. Phaser crystallographic software. J. Appl. Crystallogr, 40, 658–674. [PubMed: 19461840]

MCMANUS JJ., LOMAKIN A., OGUN O., PANDE A., BASAN M., PANDE J. & BENEDEK GB. 2007. Altered phase diagram due to a single point mutation in human γD-crystallin. Proc. Natl. Acad. Sci. U.S.A, 104, 16856. [PubMed: 17923670]

MICHIEL M, DUPRAT E, SKOURI-PANET F, LAMPI JA, TARDIEU A, LAMPI KJ & FINET S 2010. Aggregation of deamidated human βB2-crystallin and incomplete rescue by α-crystallin chaperone. Exp. Eye Res, 90, 688–698. [PubMed: 20188088]

MONTEITH WB, COHEN RD, SMITH AE, GUZMAN-CISNEROS E & PIELAK GJ 2015. Quinary structure modulates protein stability in cells. Proc. Natl. Acad. Sci. U.S.A, 112, 1739. [PubMed: 25624496]

PANDE A, MOKHOR N & PANDE J 2015. Deamidation of human γS-crystallin increases attractive protein interactions: Implications for cataract. Biochemistry, 54, 4890–4899. [PubMed: 26158710]

RAY NJ, HALL D & CARVER JA 2016. Deamidation of N76 in human γS-crystallin promotes dimer formation. Biochim. Biophys. Acta, 1860, 315–324. [PubMed: 26318015]

ROBINSON NE 2002. Protein deamidation. Proc. Natl. Acad. Sci. U.S.A, 99, 5283. [PubMed: 11959979]

ROBINSON NE, LAMPI KJ, SPEIR JP, KRUPPA G, EASTERLING M & ROBINSON AB 2006. Quantitative measurement of young human eye lens crystallins by direct injection fourier transform ion cyclotron resonance mass spectrometry. Mol Vis, 12, 704–11. [PubMed: 16807530]

SALUJA A, FESINMEYER RM, HOGAN S, BREMS DN & GOKARN YR 2010. Diffusion and sedimentation interaction parameters for measuring the second virial coefficient and their utility as predictors of protein aggregation. Biophys. J, 99, 2657–2665. [PubMed: 20959107]

SEREBRYANY E, YU S, TRAUGER SA, BUDNIK B & SHAKHNOVICH EI 2018. Dynamic disulfide exchange in a crystallin protein in the human eye lens promotes cataract-associated aggregation. J. Biol. Chem, 293, 17997–18009. [PubMed: 30242128]

SHARMA KK & SANTHOSHKUMAR P 2009. Lens aging: Effects of crystallins. Biochim. Biophys. Acta, 1790, 1095–1108. [PubMed: 19463898]

SRIVASTAVA OP & SRIVASTAVA K 2003. Existence of deamidated αB-crystallin fragments in normal and cataractous human lenses. Mol Vis [Online], 9.

TAKATA T, OXFORD JT, DEMELER B & LAMPI KJ 2008. Deamidation destabilizes and triggers aggregation of a lens protein, βA3-crystallin. Protein Sci, 17, 1565–1575. [PubMed: 18567786]

TAKATA T, SMITH JP, ARBOGAST B, DAVID LL & LAMPI KJ 2010. Solvent accessibility of βB2-crystallin and local structural changes due to deamidation at the dimer interface. Exp. Eye Res, 91, 336–346. [PubMed: 20639133]

TAKEMOTO L & BOYLE D 2000. Increased deamidation of asparagine during human senile cataractogenesis. Mol Vis, 6, 164–8. [PubMed: 10976112]

TERWILLIGER TC, GROSSE-KUNSTLEVE RW, AFONINE PV, MORIARTY NW, ZWART PH, HUNG L-W, READ RJ & ADAMS PD 2008. Iterative model building, structure refinement and density modification with the phenix autobuild wizard. Acta Crystallogr., Sec. D., 64, 61–69.

TOYAMA BH & HETZER MW 2012. Protein homeostasis: Live long, won't prosper. Nat. Rev. Mol. Cell. Biol, 14, 55.

VETTER CJ, THORN DC, WHEELER SG, MUNDORFF C, HALVERSON K, WALES TE, SHINDE U, ENGEN JR, DAVID LL, CARVER JA & LAMPI KJ 2020. Cumulative deamidations of the major lens protein γS-crystallin increase its aggregation during unfolding and oxidation. Protein Sci.

WANG J, ZUO X, YU P, BYEON I-JL, JUNG J, WANG X, DYBA M, SEIFERT S, SCHWIETERS CD, QIN J, GRONENBORN AM & WANG Y-X 2009. Determination of multicomponent protein structures in solution using global orientation and shape restraints. J. Am. Chem. Soc, 131, 10507–10515. [PubMed: 19722627]

WARMACK RA, SHAWA H, LIU K, LOPEZ K, LOO JA, HORWITZ J & CLARKE SG 2019. The l-isoaspartate modification within protein fragments in the aging lens can promote protein aggregation. J. Biol. Chem, 294, 12203–12219. [PubMed: 31239355]

WHITLEY MJ, XI Z, BARTKO JC, JENSEN MR, BLACKLEDGE M & GRONENBORN AM 2017. A combined NMR and SAXS analysis of the partially folded cataract-associated V75D γD-crystallin. Biophys. J, 112, 1135–1146. [PubMed: 28355541]

WILLIAMSON MP 2013. Using chemical shift perturbation to characterise ligand binding. Prog. Nucl. Magn. Reson. Spectrosc, 73, 1–16. [PubMed: 23962882]

WILMARTH PA, TANNER S, DASARI S, NAGALLA SR, RIVIERE MA, BAFNA V, PEVZNER PA & DAVID LL 2006. Age-related changes in human crystallins determined from comparative analysis of post-translational modifications in young and aged lens: Does deamidation contribute to crystallin insolubility? J. Proteome Res, 5, 2554–2566. [PubMed: 17022627]

ZHAO H, BROWN PH, MAGONE MT & SCHUCK P 2011a. The molecular refractive function of lens γ-crystallins. J. Mol. Biol, 411, 680–699. [PubMed: 21684289]

ZHAO H, MAGONE MT & SCHUCK P 2011b. The role of macromolecular crowding in the evolution of lens crystallins with high molecular refractive index. Phys. Biol, 8, 046004. [PubMed: 21566271]

Highlights

- NMR data reveals minimal effects of N deamidation on γD-crystallin structure
- Crystal structures of N124D and N160D are consistent with NMR results
- Deamidation does not alter the colloidal or thermodynamic stability of γD-crystallin

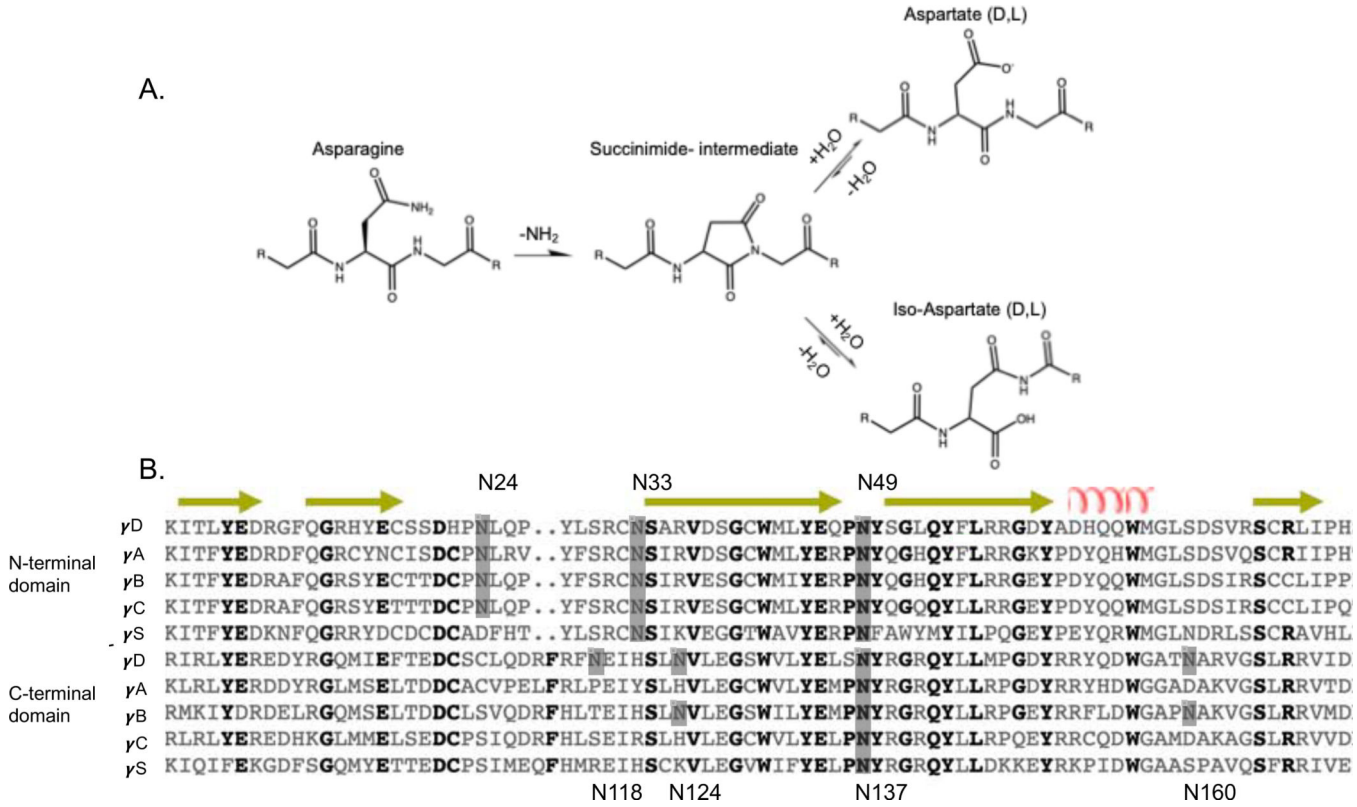

Figure 1A:

Deamidation pathway of asparagine residues. 1B: Amino acid sequence alignment of γ-crystallins. Three of the seven Asn residues are strictly conserved

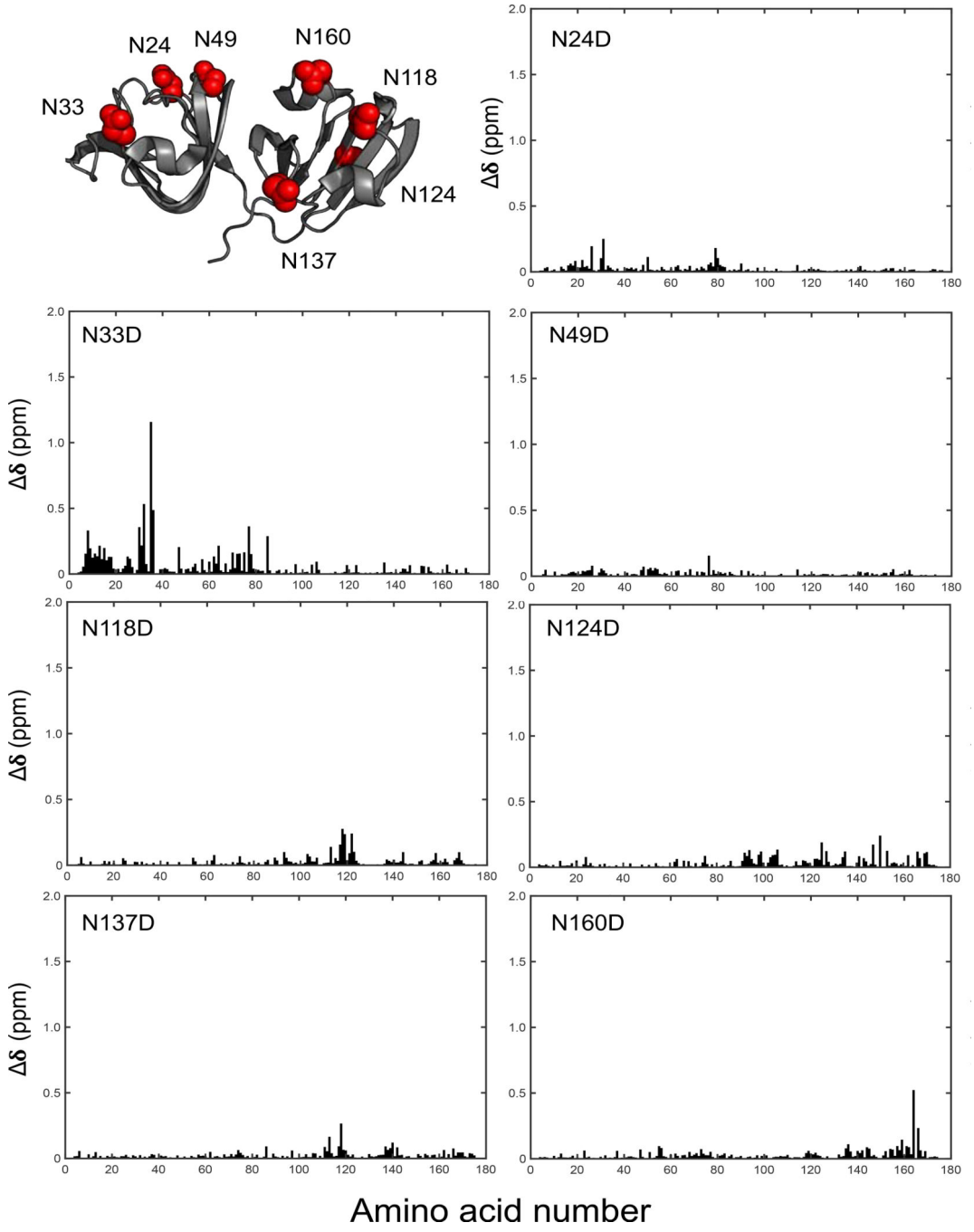

Figure 2:

Overall structure of wild-type γD-crystallin in ribbon representation with all asparagine side chains depicted in red space filling representation (top left) and amide chemical shift changes of deamidation variants, relative to wild-type γD-crystallin. Only small changes are observed, except for N33D, which exhibits larger changes close to the mutation site.

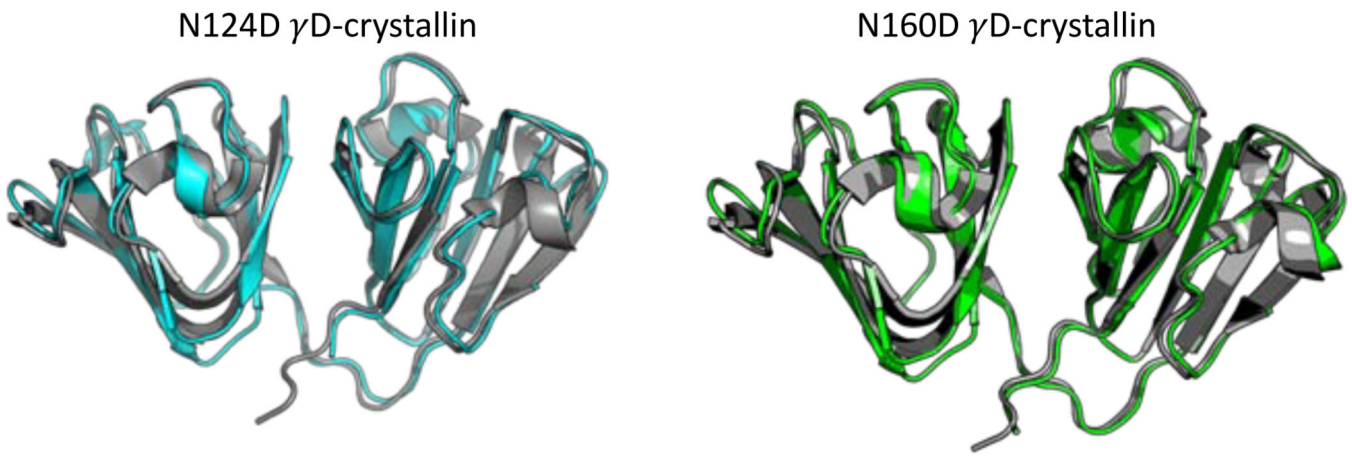

Figure 3:
Structures of N124D (cyan) and N160D (green) γD-crystallin variants in ribbon representation, superimposed on the wild-type structure (PDB 1HK0, gray).

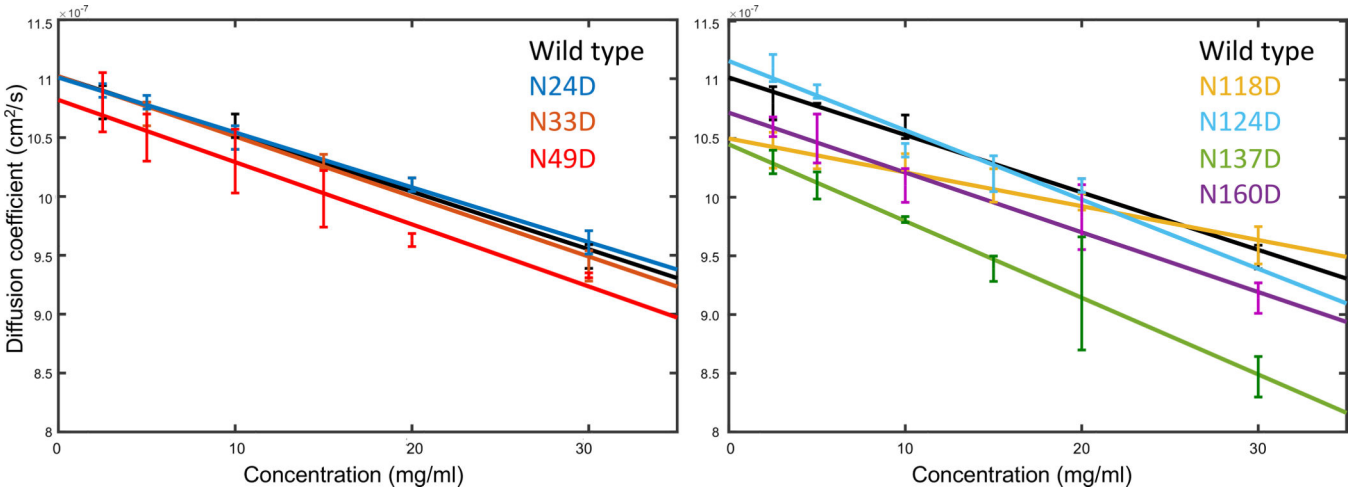

Figure 4:

Concentration dependence of the diffusion coefficient determined by DLS for wild-type and deamidation variants of γD-crystallin. The diffusion interaction parameter for each variant can be calculated from the slope of the best-fit line.

Table 1.

X-ray Data Collection and Refinement Statistics

	N124D γD-Crystallin	N160D γD-Crystallin
PDB Code	6W5B	6WCY
Data Collection		
Wavelength (Å)	0.8856	1.0
Space Group	$P2_12_12_1$	$P2_12_12_1$
Unit Cell Lengths (Å)	33.65, 51.49, 93.79	50.81, 51.87, 113.99
Unit Cell Angles (˚)	90, 90, 90	90, 90, 90
Unique Reflections	58,473	85,435
Multiplicity	11.6	12.9
Completeness (%)	99.3 (93.9)	90.9 (52.5)
Mean I/σ(I)	17.4 (2.2)	22.50 (1.0)
Wilson B-factor	12.4	17.3
R_{merge}	0.068 (0.519)	0.053 (1.185)
R_{meas}	0.071 (0.575)	0.055 (1.324)
R_{pim}	0.020 (0.241)	0.015 (0.568)
$CC_{1/2}$	0.999 (0.963)	0.999 (0.450)
Refinement		
Resolution Range (Å)	28.17 – 1.15	34.59 – 1.20
Molecules per ASU	1	2
R_{work}, R_{free}	0.151, 0.173	0.169, 0.195
CC_{work}, CC_{free}	0.963, 0.959	0.971, 0.967
Number of Non-H Atoms		
Macromolecules	1,482	2,911
Water	193	351
RMS (bonds)	0.011	0.009
RMS (angles)	1.48	1.21
Ramachandran favored (%)	98.21	99.41
Ramachandran allowed (%)	1.79	0.29
Ramachandran outliers (%)	0.0	0.29
Average B-factor		
Macromolecules	16.6	21.7
Water	28.4	31.4

Values in parentheses refer to the highest-resolution shell. The set of free reflections for R_{free} and CC_{free} were calculated with 5% of the total reflections, and these reflections were not included in the model building and refinement process.

Table 2:

Melting temperatures (T_m) determined by differential scanning calorimetry.

Variant	T_m (°C)
Wild-type	81.2
N24D	83.4
N33D	82.1
N49D	81.8
N118D	83.2
N124D	81.3
N137D	80.4
N160D	85.5

Table 3:

Diffusion interaction parameters determined by dynamic light scattering.

Variant	DIP (mL/g)
Wild-type	−4 ± 1
N24D	−5 ± 1
N33D	−4.2 ± 0.5
N49D	−5 ± 1
N118D	−3 ± 1
N124D	−5 ± 2
N137D	−6 ± 1
N160D	−5 ± 2

Key Resources Table

REAGENT or RESOURCE	SOURCE	IDENTIFIER
Bacterial and Virus Strains		
Escherichia coli BL21(DE3)	NEB	Cat# C2527H
Chemicals, Peptides, and Recombinant Proteins		
Tris	Fisher	Cat# 61202–5000
MES	Sigma	Cat#5287
EDTA	Fisher	Cat#AAJ15694AE
TCEP	Sigma	Cat#C4706
DTT	RPI	Cat#D11000
NaCl	Sigma	Cat#S7653
^{15}N NH_4Cl	Cambridge isotope labs	Cat#NLM-467
D_2O	Cambridge isotope labs	Cat#DLM-4
IPTG	RPI	Cat#I56000
Deposited Data		
Crystal structure of γD-crystallin	Basek et al 2003	PDB: 1HK0
NMR Structure of γD-crystallin	Wang et al 2009	PDB: 2KLJ
Crystal structure of N124D γD-crystallin	This paper	PDB: 6W5B
Crystral structure of N160D γD- crystallin	This paper	PDB: 6WCY
Recombinant DNA		
pET14b CRYGD	Ji et al 2012	N/A
Modified pET14b vectors	This paper	N/A
Software and Algorithms		
NMRFAM-SPARKY	Lee et al 2014	https://nmrfam.wisc.edu/nmrfam-sparky-distribution/
Phaser	McCoy et al 2007	https://www.ccp4.ac.uk
COOT	Emsley et al 2004	https://www2.mrc-lmb.cam.ac.uk/personal/pemsley/coot/
Phenix AutoBuild	Terwilliger et al 2008	https://www.phenix-online.org/documentation/reference/autobuild.html
Origin	Malvern	N/A
Phenix	Adams et al 2010	https://www.phenix-online.org
PyMol	Schrödinger	https://pymol.org/2/
protSA	Estrada et al 2009	http://webapps.bifi.es/ProtSA/
Matlab	Mathworks	N/A
Dynamics 7.1.7	Wyatt Technologies	N/A
Other		
384-well DLS plate	Corning	Cat#3540
HiTrap Q HP	GE Healthcare	Cat#17115401
HiTrap HP SP	GE Healthcare	Cat# 17115201
Amicon Spin Concentator 10000 MWCO	Amicon	Cat# UFC901024
HiLoad 16/600 Superdex 75 pg	GE Healthcare	Cat#28989333